

VALIDATION OF DEM PREDICTIONS OF GRANULAR FLOW AND SEPARATION EFFICIENCY FOR A HORIZONTAL LABORATORY SCALE WIRE MESH SCREEN

Gary W. DELANEY¹, Paul W. CLEARY¹, Marko HILDEN² and Rob D. MORRISON²

¹CSIRO Mathematical and Information Sciences, Private Bag 33, Clayton South, 3168, Australia

²Julius Kruttschnitt Mineral Research Center, the University of Queensland, Isles Rd, Indooroopilly, Qld, 4068, Australia.

ABSTRACT

Large scale industrial screens are used extensively in separating particles by size into multiple product streams. Their performance in terms of throughput and screening efficiency is of vital economic and industrial importance, as in many applications this can be a limiting factor in the overall efficiency of multi-step industrial processes. Discrete Element Method (DEM) predictions of flow and separation efficiency using spherical particles are compared to experimental data in order to assess their accuracy. The apparatus consists of a laboratory scale horizontal screen with a wire mesh cloth onto which quarry rock is feed at a series of flow rates. The screen is vibrated causing the granular bed to flow over the deck and causing it to vertically stratify with finer material passing through the screen to be collected below for analysis. Product mass and size distribution data is collected in a series of bins located along the length of the screen allowing a detailed understanding of the progress of the separation to be developed.

INTRODUCTION

Screening processes in which particles are separated according to size are important in a wide range of industrial activities. These range from processing of iron ore, coal and other minerals, to the production of food and pharmaceuticals. Until recently, most studies of screening behavior were either experimental or theoretical. Standish *et al.* (1986) carried out experiments studying the behavior of a vibrating screening setup for a range of operating variables including feed rate, deck angle and screen mesh size. A kinetic approach was used to analyze the data and the screening behavior of the individual particle sizes was related to the particles' kinetic constants. Nakajima and Whiten (1979) investigated the effect of particle shape on screening behavior and developed an empirical probability function to give the fractional recovery of non-spherical particles in the oversize for rectangular aperture screens. Deghani *et al.* (2002) improved on this work by replacing the empirical function in the Nakajima model with a probability equation depending on particle dimensions.

Numerical modeling using the Discrete Element Method (DEM) has recently been shown to be a useful tool in examining how the screening performance is affected by a number of different factors, potentially allowing for effective optimization strategies to be determined. Cleary and Sawley (2002) employed DEM with spherical particles to perform three-dimensional simulations of screening on vibrating decks. This demonstrated the ability of DEM to simulate these kinds of granular flows and the method's potential for use as a design tool for industrial particle handling equipment.

Cleary *et al.* (2004) further demonstrated how the effect of particle shape can be taken into account in such DEM simulations and even be applied to the investigation of complex full-size industrial screens, such as the performance of double deck banana screens (Cleary *et al.*, 2009a). It was found that for these multi-decked curved screen setups an optimal screen acceleration should balance two key competing factors in the screening performance, that of dilating the granular bed to aid the percolation of fine particles (favored by high accelerations) and allowing the opportunity for the fine particles near the screen surface to be captured by the screen apertures (favored by low accelerations). It was also shown that DEM could be used to make quantitative predictions and determine the stress and wear on the individual screen cloths (Cleary *et al.*, 2009b). Dong *et al.* (2009) has used a spherical DEM model to consider particle flow on a five progressively shallower slotted panels, investigating the effects of operational conditions and geometry on performance.

In this work we will consider a vibrated horizontal screening apparatus and compare simulation results using DEM with experimentally obtained data. Our simulations are setup to match the experimental apparatus geometry, input feed rate and vibration conditions. In the DEM model used here, we will just consider spherical particles. We will compare against experimentally obtained data and determine the areas in which the spherical DEM model can effectively predict screening performance for real industrial screens. Where good agreement is not found, we suggest appropriate model refinements.

EXPERIMENTAL SETUP

A series of screening experiments were carried out using a laboratory scale horizontal screening apparatus. The apparatus was 90 cm long and 15cm wide and had a series of 8 collection bins (first four 9 cm long, last four 18 cm long) placed underneath and an overflow bin at the end of the screen (See Figure 1). The screen wire was 0.71 mm in diameter and the aperture size was 3.52 mm. The screen was vibrated at an amplitude of 1.76 mm at a frequency of 27.55 Hz with a stroke angle to the horizontal of 50°, giving a G-force value of 2.69. Quarry rock with a density of 2700 kg/m³ was used. A series of experiments at feed rates ranging from 0.05 kg/s to 0.25 kg/s were performed. The material was fed onto the input end of the screen using a pan feeder and the experiment was run until all material had been screened into either a collection bin or the overflow bin at the end of the screen. To analyse the size distribution of the particles in each bin, the collected material was repeatedly weighed and then screened through a series of successively finer screens with apertures ranging from 4.75 mm to 0.6 mm.

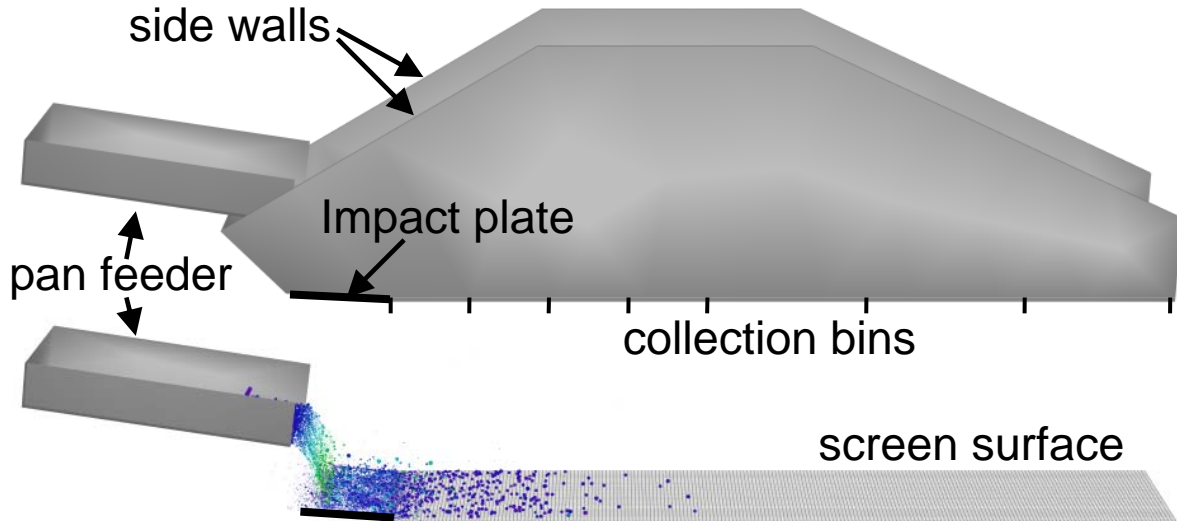


Figure 1: CAD model of the configuration used in the experiments and simulations. The top image shows the setup with the side walls in place. The bottom image has the side walls removed so that the screen surface is visible. A flow of particles is fed onto the impact plate from a pan feeder and then flows onto the screen surface due to its vibration.

SIMULATION DETAILS

DEM is a numerical technique for simulating the motion of collections of individual particles (Cundall and Strack, 1979). It has been used extremely successfully in many areas of science, and has been applied to the simulation of bulk materials, powders and a large variety of granular matter including sand, cereals and soil (Cleary et al., 2004, Cleary 2009; Hutzler et al., 2004). In DEM, each particle is tracked and all collisions between particles and between particles and boundaries are modelled. The particles are allowed to overlap and the extent of overlap is used in conjunction with a contact force law to give instantaneous forces from knowledge of the current positions, velocities and spins of the particles. We use spherical particles and a linear spring-dashpot model which takes account inelasticity and frictional contributions. Further details of the model are given in references (Cleary 2004; Cleary et al. 2009a).

Screen length	90 cm
Screen width	15 cm
Deck slope	0°
Aperture size	3.52 mm
Wire diameter	0.71 mm
Vibration Amplitude	1.76 mm
Vibration Frequency	27.6 Hz
G-force	2.69
Angle of Stroke	50

Table 1: Summary of screen geometry and motion.

A CAD model was constructed, exactly matching the structure and dimensions of the experimental system (see Figure 1). This was then used in DEM simulations that were set up to match the experimental system. Table 1 gives a summary of the geometric details of the screen and its motion. The screen surface consisted of a square hole

wire mesh with square opening dimension 3.52 mm and a wire diameter of 0.71 mm.

The particle size distributions for each experiment are given in Table 2 and the distribution used in each simulation matches this. The coefficient of restitution for collisions between particles was 0.4 and between particles and the screen was 0.5. The friction coefficient for collisions between particles and between particles and the screen was 0.5. The spring stiffness used was 1000 N/m which gave average overlaps of around 0.5% of the smallest particle diameter.

Top Size (mm)	Class i.d.	Feed Rate 0.05kg/s	Feed Rate 0.125kg/s	Feed Rate 0.25 kg/s
5.00	1	3.1%	4.97%	3.10%
4.75	2	5.6%	7.92%	6.01%
4.00	3	9.7%	16.93%	12.64%
3.35	4	11.1%	22.07%	19.79%
2.80	5	7.7%	12.38%	11.83%
2.36	6	12.0%	12.33%	12.47%
2.00	7	8.6%	9.22%	9.99%
1.70	8	6.4%	6.32%	6.51%
1.40	9	5.3%	3.27%	4.67%
1.18	10	6.8%	2.15%	4.53%
1.00	11	5.4%	1.32%	3.19%
0.85	12	4.2%	0.75%	2.17%
0.71	13	3.6%	0.28%	1.21%
0.60	14	10.4%	0.11%	1.90%

Table 2: Particle size distributions measured from the experimental system and used in the simulations. The upper-size for each size class is given in the first column, with the bottom size of each class given in the row below. The bottom size of the last class is 0.5 mm.

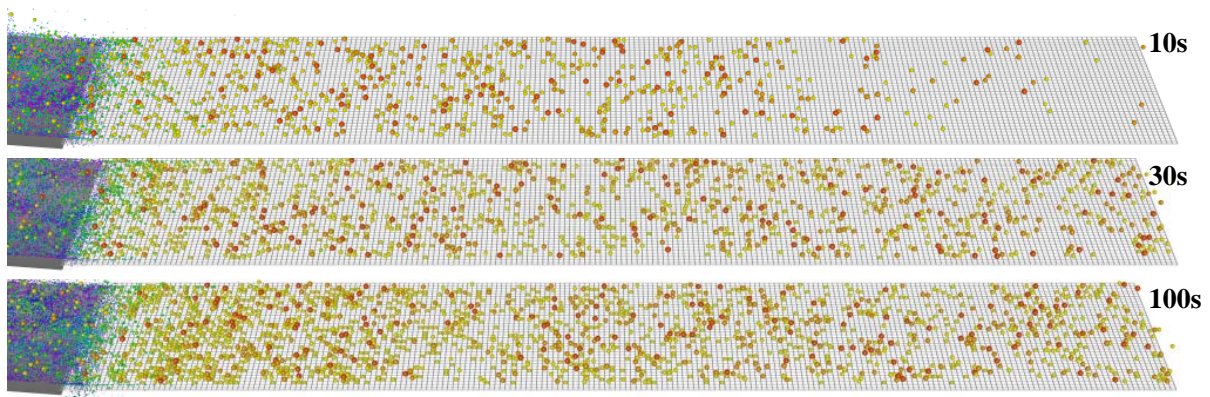


Figure 2: Flow over the screen for feed rate 0.05 kg/s at $t = 10$ s (top), 30 s (middle) and 100 s (bottom). The particles are coloured by size, with blue being the smallest and red being the largest. The system very quickly stabilizes with material smaller than the screen aperture size rapidly falling through the cloth near the start of the screen.

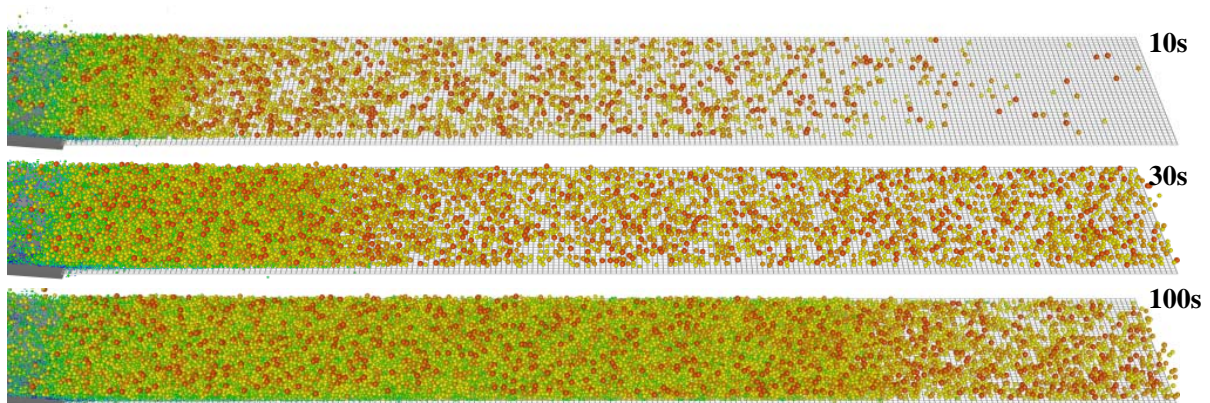


Figure 3: Flow over the screen for feed rate 0.125 kg/s at $t = 10$ s (top), 30 s (middle) and 100 s (bottom). The particles are coloured by size, with blue being the smallest and red being the largest.

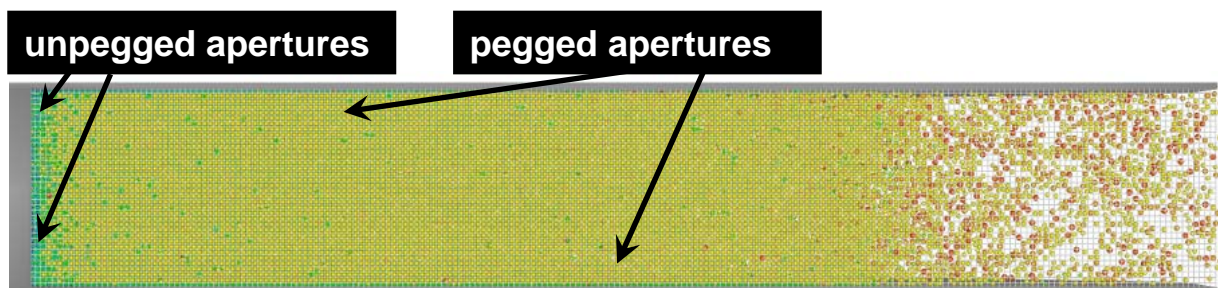


Figure 4: Underside of the screen for the mid feed rate of 0.125 kg/s at $t = 100$ s. The apertures of the screen become pegged by the near aperture sized material (coloured yellow) blocking the holes and inhibiting screening. There is a small region at the start of the screen, just after the impact plate, where there is very little pegging.

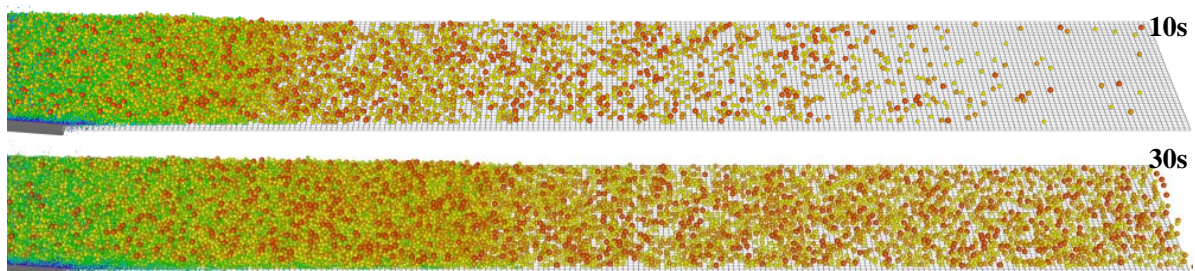


Figure 5: Flow over the screen for feed rate 0.250 kg/s at $t = 10$ s (top) and 30 s (bottom). The particles are coloured by size, with blue being the smallest and red being the largest.

A stream of particles with the same size distribution and feed rate as used in the experiment was fed onto the screen using a pan feeder. A series of data collection bins were setup at contiguous intervals under the screen and an overflow bin at the end of the screen to match the bins used in the experiment. The mass of the particles in each size class was determined and compared to the corresponding experimental value.

FLOW OVER THE SCREEN

Figure 2 shows images of the low feed rate case of 0.05 kg/s at $t = 10$ s, 30 s and 100 s. Particles enter from the left and the smaller particles (blue) quickly fall through the screen openings. The stream of particles on the top of the cloth rapidly coarsens (shown by the increasing red coloration) as the fine particles fall through. After an initial equilibration period, the screening behaviour appears reasonably constant, with the majority of the material below the screen aperture size being quickly captured into the first collection bin under the screen and the remaining over-sized particles forming a dilute flow over the rest of the screen. Progress of the dilute coarse material can be seen at $t = 30$ s and 100 s.

For the intermediate feed rate of 0.125 kg/s, we see a very different behaviour. There is a visibly larger amount of material entering the screen (Figure 3) from the left. The majority of the finest material is again quickly captured into the first collection bin. The screening of the mid-large sized material (green, yellow and red) is now severely inhibited and we see an increasing build up of this material on the screen as we go from $t = 10$ s to 100 s. The main cause of this build up is due to “pegging”, where the holes in the wire screen mesh become blocked by particles whose diameters are close to the screen aperture size. This is a result of the use of spherical particles in the

simulation, which can very readily peg the screen apertures and inhibit subsequent flow through the screen. Figure 4 shows the underside of the screen at $t = 100$ s. There is a region approximately five apertures wide at the start of the screen, just after the impact plate, where there is very little pegging. The flow of the grains from the feeder and along the impact plate stratifies the bed, so that the mid-large size material is being carried along near the top of the bed and above the finer material as it enters the screen from the impact plate. This means that there are few mid-large size particles near the start of the screen surface and thus they cannot easily peg this early region of the screen. The majority of the fine material is collected in the first bin as the bed flows over the start of the screen. As the finer material falls from the bed, the coarser material above moves lower. Once the mid-sized particles reach the surface of the screen they are able to start pegging the parts of the screen beyond that point. After this initial section of the screen, we see that there is a wide region in which nearly all of the screen apertures have become pegged and this region grows with time as the near aperture sized material is forced to travel further along the screen by the already pegged (and therefore impermeable) part of the screen.

Figure 5 shows the high feed rate case of 0.25 kg/s at $t = 10$ s and 30 s. We see a very similar behaviour to that of the 0.125 kg/s rate. Pegging is again the key effect which determines the screening behaviour, causing a rapid build up of the material on the screen due to the screen apertures becoming blocked. The larger feed rate causes this build up to occur more quickly than for the mid feed rate case. This can be seen by the larger amount of material present on the screen at $t = 30$ s. Following the pegged region, there is again a relatively dilute flow of the larger material (red and yellow) over the remainder of the screen.

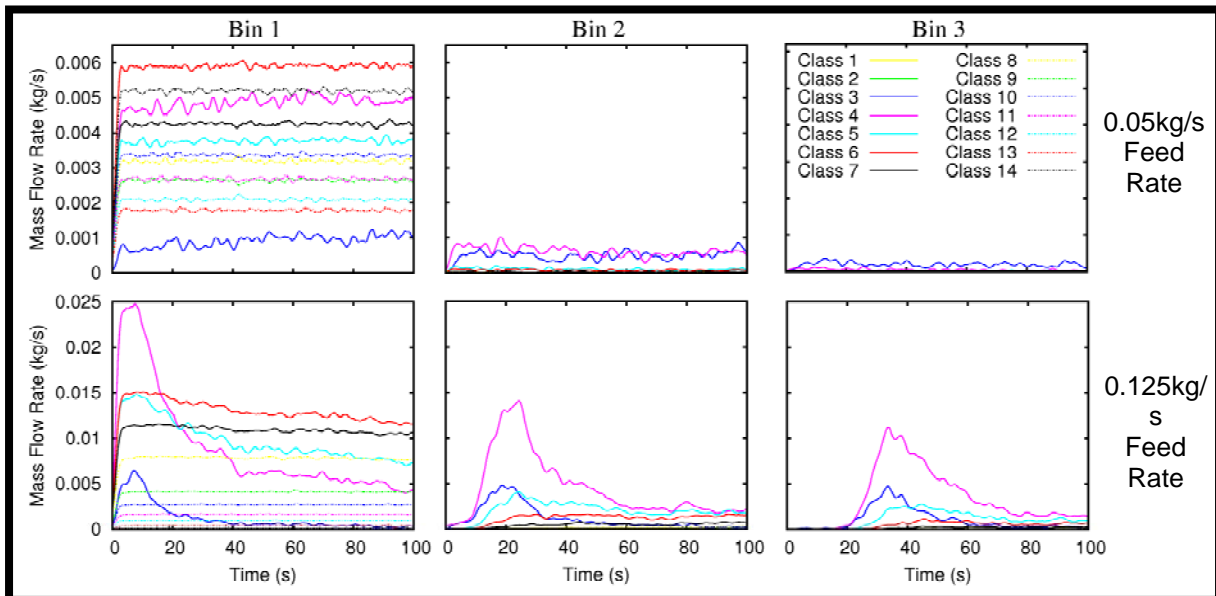


Figure 6: Flow rates through the first, second and third collection bins, for feed rates of 0.05 kg/s and 0.125 kg/s. The numbered classes correspond to those described in Table 2.

FLOW THROUGH THE SCREEN

Figure 6 shows the mass flow rates for each of the size classes into the first three collection bins under the screen for the low (0.05 kg/s) and mid (0.125 kg/s) feed rates. For the low feed rate case, after the initial time for the flow to reach the screen, the mass flow rates into the collection bins are reasonably constant with time for each size class. The first bin captures almost all of the fine material, with classes 5-14 (mid-fine sized material) having almost zero flow rates into the following bins. Class 4 mainly flows into the first 2 bins, with its flow rate into the second bin being about 25% of the rate into the first. The near aperture sized material (Class 3) has appreciable flow rates into the all 3 collection bins, with the flow into the second and third bins being about 75% and 25% of the flow rate into the first. For the 0.125 kg/s feed rate case, the flow rates for the finer material (classes 7-14) are constant with time (see Figure 6b) and are largely captured in the first bin under the screen. However, the flow rates for the intermediate size classes (that are still below the screen aperture size) show significant time dependence. This is most apparent for size classes 3, 4 and 5 (represented by the dark blue, aqua and pink lines in Figure 6) where the flow rate into the first bin declines significantly after 7-8 s. There are corresponding increases in the flow into the second bin. This is due to the pegging effects, which block increasing numbers of the holes over the first bin. Mid-sized material is then unable to pass through this part of the screen and therefore travels further along the screen to reach unpegged holes, which are by then over the second bin. This process continues with the holes above each subsequent bin becoming increasingly pegged, causing the capturing of the mid-sized material to move to bins located increasingly further along the screen. This same behaviour is also found for the higher 0.25 kg/s feed rate.

COMPARISON WITH EXPERIMENT

Low feed rate case

Figure 7a shows the fractions of the total collected mass contained in each bin under the screen for both simulation and experiment. For the low feed rate, the majority of the material in the experiment is captured in the first collection bin (90%). A small amount of material (5%) is collected in the second bin, and then virtually no material is captured in the subsequent bins. This is due to the very dilute flow allowing very effective screening into the first collection bin. The simulation predicts a very similar pattern of discharge but has a slightly higher fraction (about 3% more) being captured by the first bin.

Figure 7b shows the fractions of the total collected mass that are in each class in the first bin. A significantly larger fraction of the near aperture sized material (classes 3-5) is collected in the simulation than in the experiment. This accounts for the over-prediction in the mass fraction seen in the first bin in Figure 7a. This means that near aperture size particles are much more able to pass through the screen than are the equivalent real particles.

Figure 7c shows the fraction of the each class's mass that is collected in the first bin. The mid to fine sizes (classes 6-14) are nearly 100% captured in the first bin for both the simulation and experiment. For the coarser

near aperture size particles (classes 3-5), much larger fractions are captured in the first collection bin in the simulation than in the experiment, with four times as much in class 3 and twice as much in class 4. The coarsest particles (classes 1 and 2) cannot pass through the screen and so are not represented.

The near aperture sized particles clearly flow more easily through the screen than those in the experiment. This can be attributed to the shape of the particles. The critical particle dimension for screening particles with a non-unit aspect ratio is expected to be some combination of its intermediate and smaller semi-major axes. The long axis of a non-round particle will be bigger than this dimension. Such a particle flowing along above the screen will tend to have its long axis parallel to the screen surface but needs to have its long axis pointing into one of the holes in the screen in order to be trapped by it. The particle then needs to work its way through that hole without being pulled out and along by the flowing bed above. In contrast, a spherical particle with a diameter equal to the characteristic dimension of the non-round particle can much more easily be trapped by the hole in the screen and more easily pass through it. The non-round nature of a particle therefore sharply reduces the chances of a near aperture size particle being trapped by the screen and also increases its transit time through the screen. There is also a higher chance of an elongated particle being dislodged by the flowing particles around it. For these reasons one would expect a round particle to have a much higher chance of passing through any particular hole and will lead to an overall increased fraction of these particles reporting to the first bin.

Mid and high feed rate cases

We have seen in the previous sections that the use of spherical particles leads to large amounts of pegging and a resulting reduction of the flow rates into the collection bins as the apertures become blocked. This makes the separation data for each bin time dependent, with first an increase in the flow rate, followed by a decrease as the holes above each bin become blocked. It appears that the only steady state condition that will be reached is an almost entirely pegged screen with all holes blocked, except for a short section at the start of the screen. This is not a realistic representation of the experimental system, where the real particles do not generate these severe pegging effects.

The time dependence caused by pegging can be seen in Figure 8 where we consider the fraction of mass collected in each bin at three different time frames during the simulation: $t = 0-30$ s, $30-60$ s and $60-100$ s for 0.125 kg/s. The fraction of the mass sampled in the first bin decreases from 85% for the 0-30 s period to 60% for the 60-100 s period. The large fraction of the mass still sampled by the first bin is due to the fine material being captured in the unpegged region at the start of the screen (as shown in Figure 4). In the experiment, the majority of the mid-fine material is also captured in this bin. The fraction of the mass captured in each of the other bins in the simulation goes through a cycle of an initial increase as the holes over the previous bin become pegged and then a decrease as its own holes

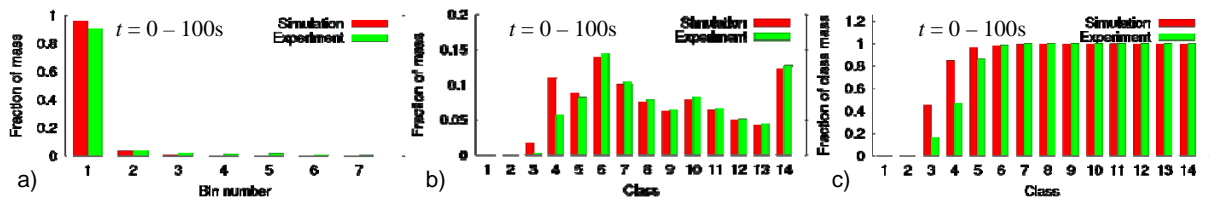


Figure 7: Comparisons between simulation and experiment for the 0.05 kg/s case over the full simulation time $t = 0 - 100$ s. The figures show a) the fractions of the total collected mass contained in each bin under the screen, b) the fractions of the total collected mass that is captured in the first collection bin in each class, and c) the fraction of each class's mass that is captured in the first collection bin.

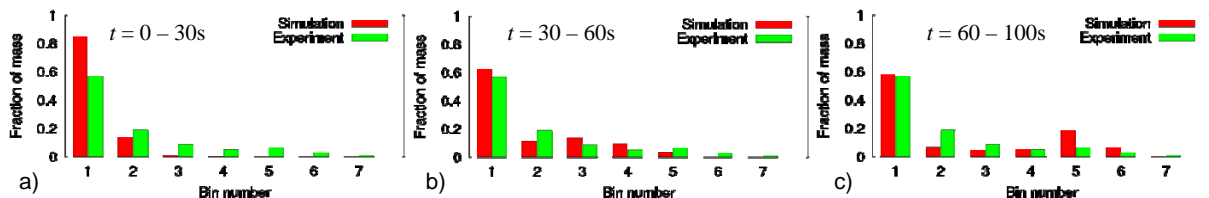


Figure 8: The figures show the fraction of mass captured in each collection bin under the screen during for the 0.125 kg/s feed rate, at three time frames during the simulation: a) $t = 0-30$ s, b) $t = 30-60$ s and c) $t = 60-100$ s. The experimental data is also plotted on each graph for comparison.

become pegged. This causes a qualitatively different behaviour to that of the experiment. This can be seen in the fraction of mass captured by the third bin increasing from about 2% during the first time period, to 12% during the second period and then back down to about 3% in the final period. The pegged region of the screen has extended up to the end of the 4th bin by this time, leading to the very high fraction of material (20%) being captured in the 5th bin

Similar time dependent behaviour, dominated by pegging, is also seen for the high feed rate.

CONCLUSION

In this work we have compared experimentally obtained data for a horizontal screen with DEM simulations using spherical particles. For the low feed rate case, we find reasonable agreement for the mid-fine size classes, which are mainly captured in the first collection bin in both the simulation and the experiment. The fraction of the mass in each size class in this bin also shows generally good agreement for the mid-fine size classes, but large differences for the near aperture sized material, which is captured at a much higher rate in the simulation than the experiment. This is attributable to particle shape effects, which allow spherical particles to more easily percolate down to the screen surface and to be captured by a screen aperture leading to over-prediction of the separation rate for these larger particles.

At higher feed rates, very significant deviations between the experiment and the simulation emerge. The behaviour of the simulation is dominated by severe pegging effects which are an artefact of using spherical particles in the simulation model. This causes a significant time dependent effect, where the screen apertures become increasingly blocked, causing the main flow of the mid size material into the collection bins to move further along the length of the screen.

In future work, we will examine the performance of the system using non-spherical particles. It is expected that this will sharply reduce the extent of pegging, and provide a more realistic percolation of the material

through the flowing bed and separation of the near aperture size material at the screen surface.

REFERENCES

- CLEARY P.W., (2004), "Large scale industrial DEM modelling", *Eng. Computations*, 21, no. 2/3/4, 169 - 204.
- CLEARY PW, SINNOTT MD, MORRISON RD. (2009), "Separation performance of double deck banana screens - Part 1: Flow and separation for different accelerations". *Minerals Eng.*; 22(14):1218-1229.
- CLEARY PW, SINNOTT MD, MORRISON RD., (2009), "Separation performance of double deck banana screens - Part 2: Quantitative predictions". *Minerals Engineering*. Nov; 22(14):1230-1244.
- CLEARY PW., (2004), "Large scale industrial DEM modeling". *Eng. Computations*. 21(2/3/4):169 - 204.
- CUNDALL P.A. AND STRACK ODL, (1979), "A discrete numerical model for granular assemblies", *Geotechnique* 29: 65, 47.
- DEHGHANI A, MONHEMIUS AJ, GOCHIN RJ. (2002), "Evaluating the Nakajima et al. model for rectangular-aperture screens". *Minerals Eng.* 15(12): 1089-1094.
- DONG K, YU A, BRAKE I., (2009), "DEM simulation of particle flow on a multi-deck banana screen". *Minerals Engineering*. Oct; 22(11):910-920.
- NAKAJIMA, Y., WHITEN, W.J., (1979), "Behaviour of non-spherical particles in screening". *Trans. Inst. Min. Metall.*; 88, C88-92.
- STANDISH N, BHARADWAJ AK, HARIRI-AKBARI G., "A study of the effect of operating variables on the efficiency of a vibrating screen". *Powder Tech.*. 1986 Oct; 48(2):161-172.
- HUTZLER S, DELANEY G, WEAIRE D, MACLEOD F., (2004) "Rocking Newton's cradle". *Am. J. Phys.* Dec 0;72,1508-1516.